

Научный семинар



materials



Article

Nanoindentation of γ -TiAl with Different Crystal Surfaces by Molecular Dynamics Simulations

Xiaocui Fan ¹, Zhiyuan Rui ^{1,2,*}, Hui Cao ¹, Rong Fu ¹, J

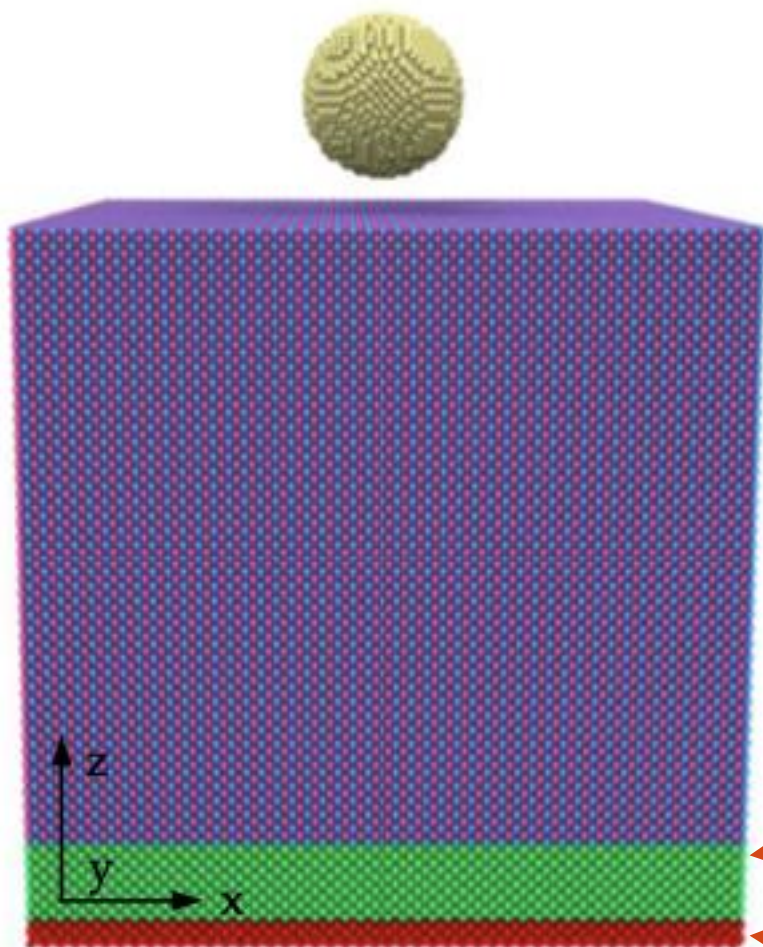
Ruicheng Feng ^{1,2}  and Changfeng Yan ^{1,2}






Постановка задачи: начальная структура

X, Y – periodic BC
Z – free BC

Релаксация в течении 380 пс при 300К



 Newtonian layer
 Thermostat layer
 Boundary layer

Слой отвечает за контроль температуры в системе

Атомы неподвижны, подложка зафиксирована

Figure 1. Nanoindentation model of γ -TiAl.



Постановка задачи: тип решетки

The crystal structures of different γ -TiAl samples are displayed in Figure 2, the base vectors x , y and z are set as $[00\bar{1}]$, $[010]$ and $[100]$ for the (100) sample (Figure 2a); $[\bar{1}\bar{1}2]$, $[111]$ and $[\bar{1}10]$ for the $(\bar{1}10)$ sample (Figure 2b); and $[\bar{1}\bar{1}2]$, $[\bar{1}\bar{1}0]$ and $[111]$ for the (111) sample (Figure 2c).

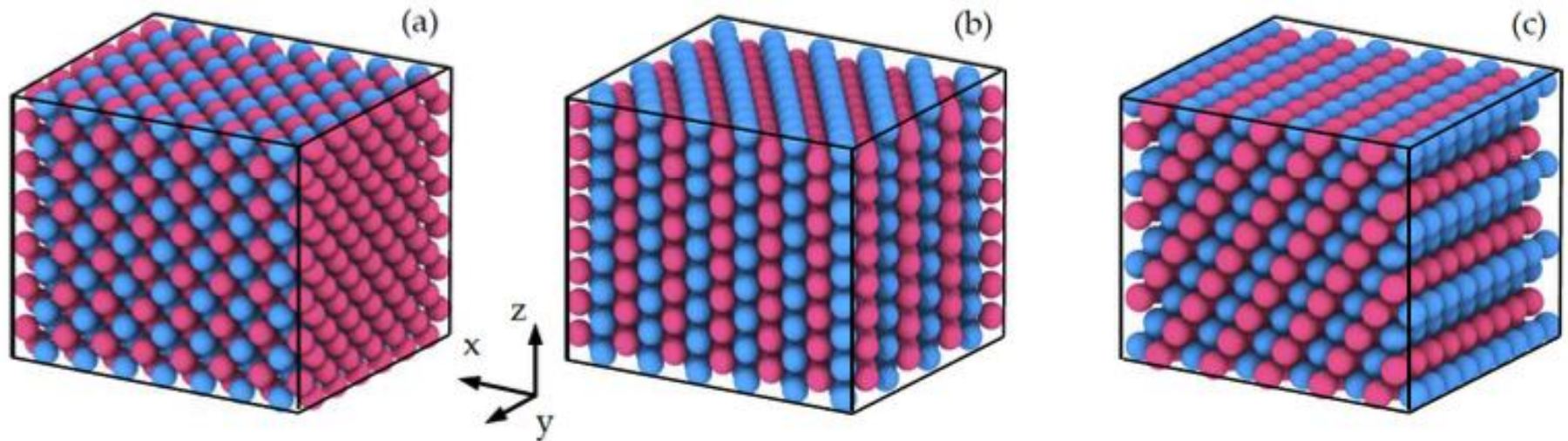


Figure 2. The crystal structure of (a) the (100) sample, (b) the $(\bar{1}10)$ sample and (c) the (111) sample. The Ti atoms are colored purple and the Al atoms are colored blue.



Постановка задачи: потенциалы

Взаимодействие Al-Ti описывается потенциалом EAM

Взаимодействием C-C пренебрегаем, поскольку индентер – жесткое целое

Взаимодействие Al-C и Ti-C опишем парным потенциалом ЛД

$$U(r) = 4\epsilon \left[\left(\frac{\sigma}{r} \right)^{12} - \left(\frac{\sigma}{r} \right)^6 \right], r < r_0$$

Table 1. Mie 6–12 (Lennard–Jones) potential function parameters used in simulation.

Parameters	σ (Å)	ϵ (10^{-1}ev)	r_0 (Å)
C-Al	2.976	3.15	7.44
C-Ti	3.759	0.314	9.398



Кривые напряжение-деформация

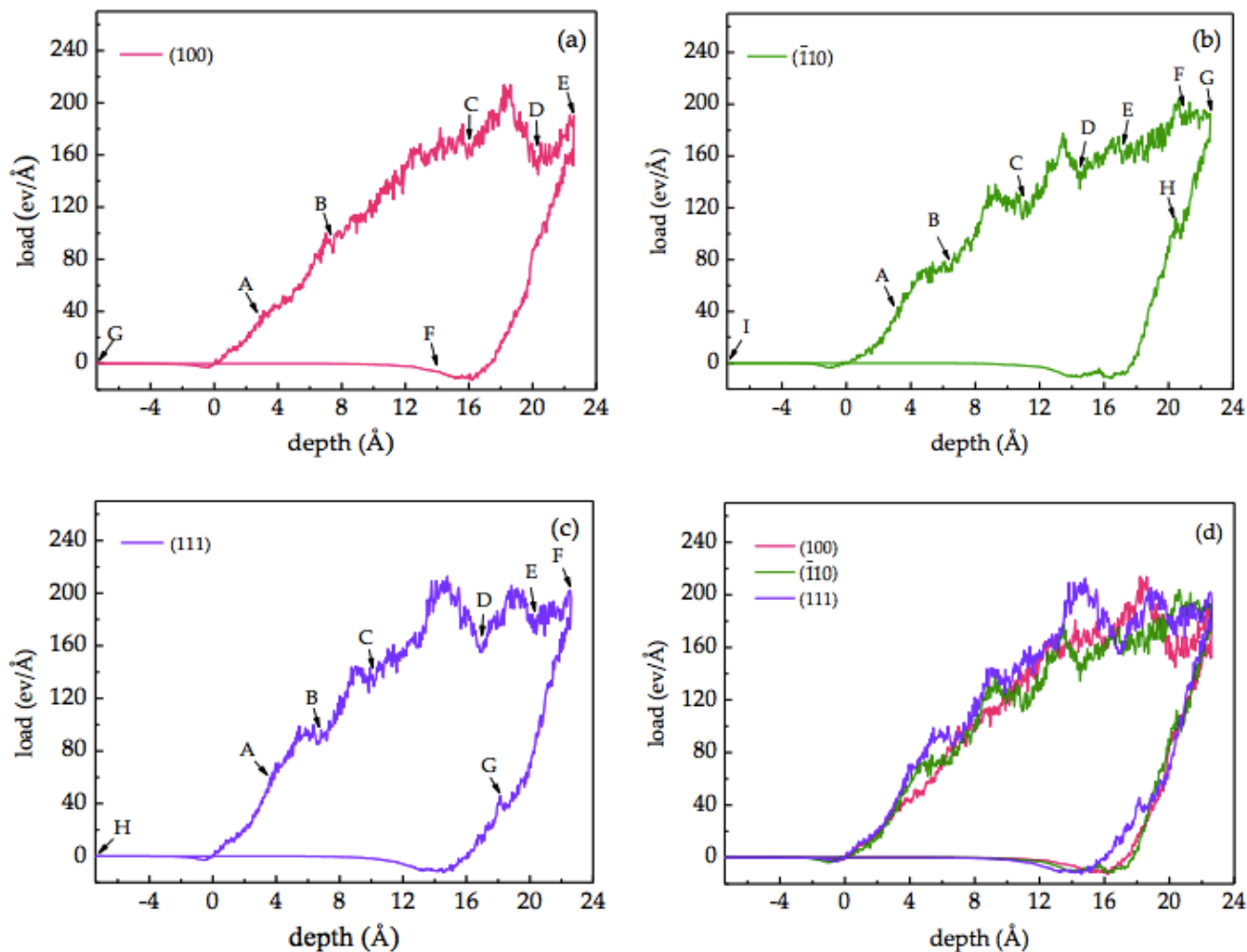


Figure 3. Load-depth curve of (a) the (100) sample, (b) the $\bar{1}\bar{1}0$ sample and the (c) (111) sample; (d) shows the load-depth curves of the three different samples. The letters labeled in (a–c) represent the characteristic points, and the defect evolution at these points will be described in Section 3.2.



Зарождение дефектов, образец (100)

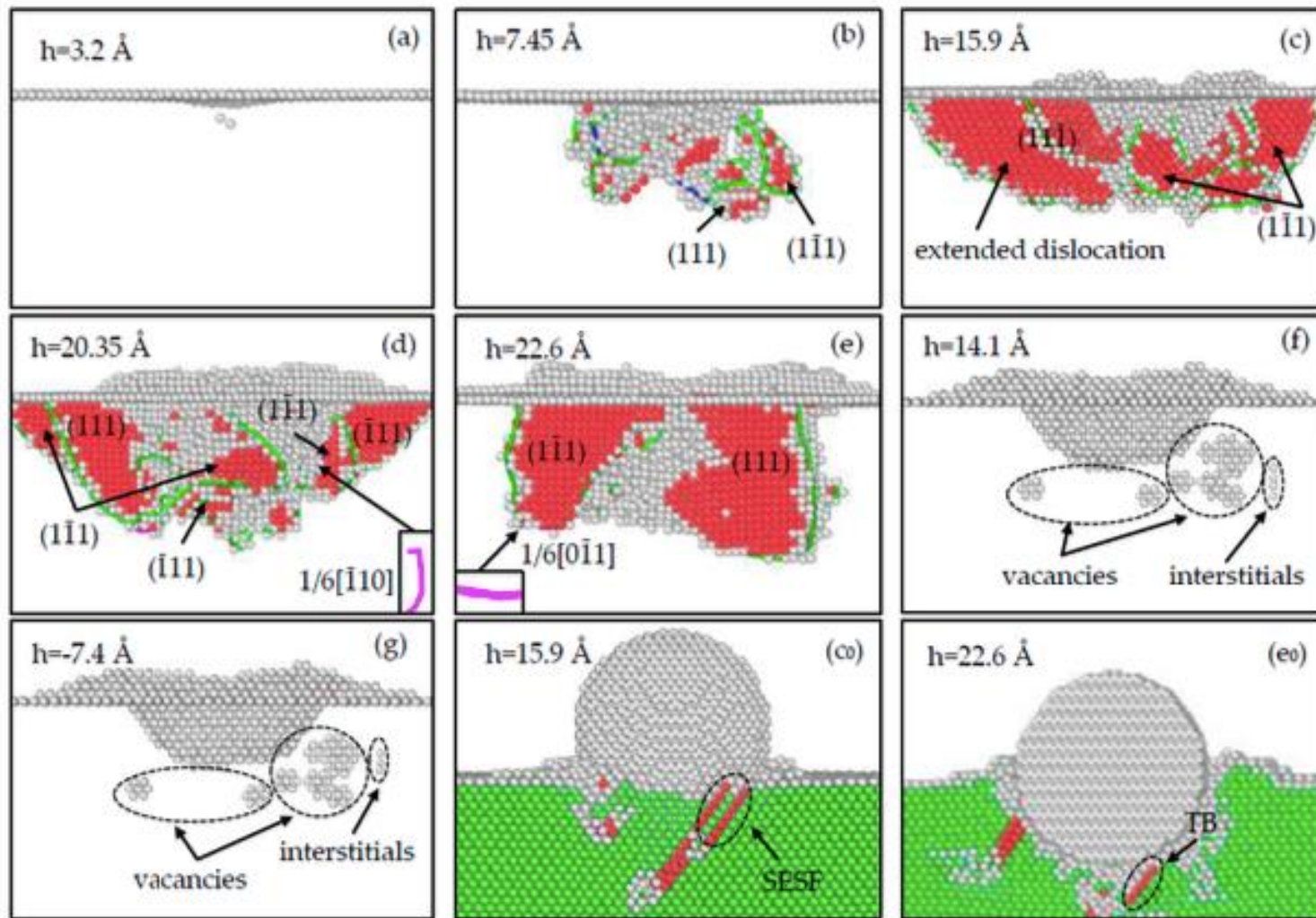
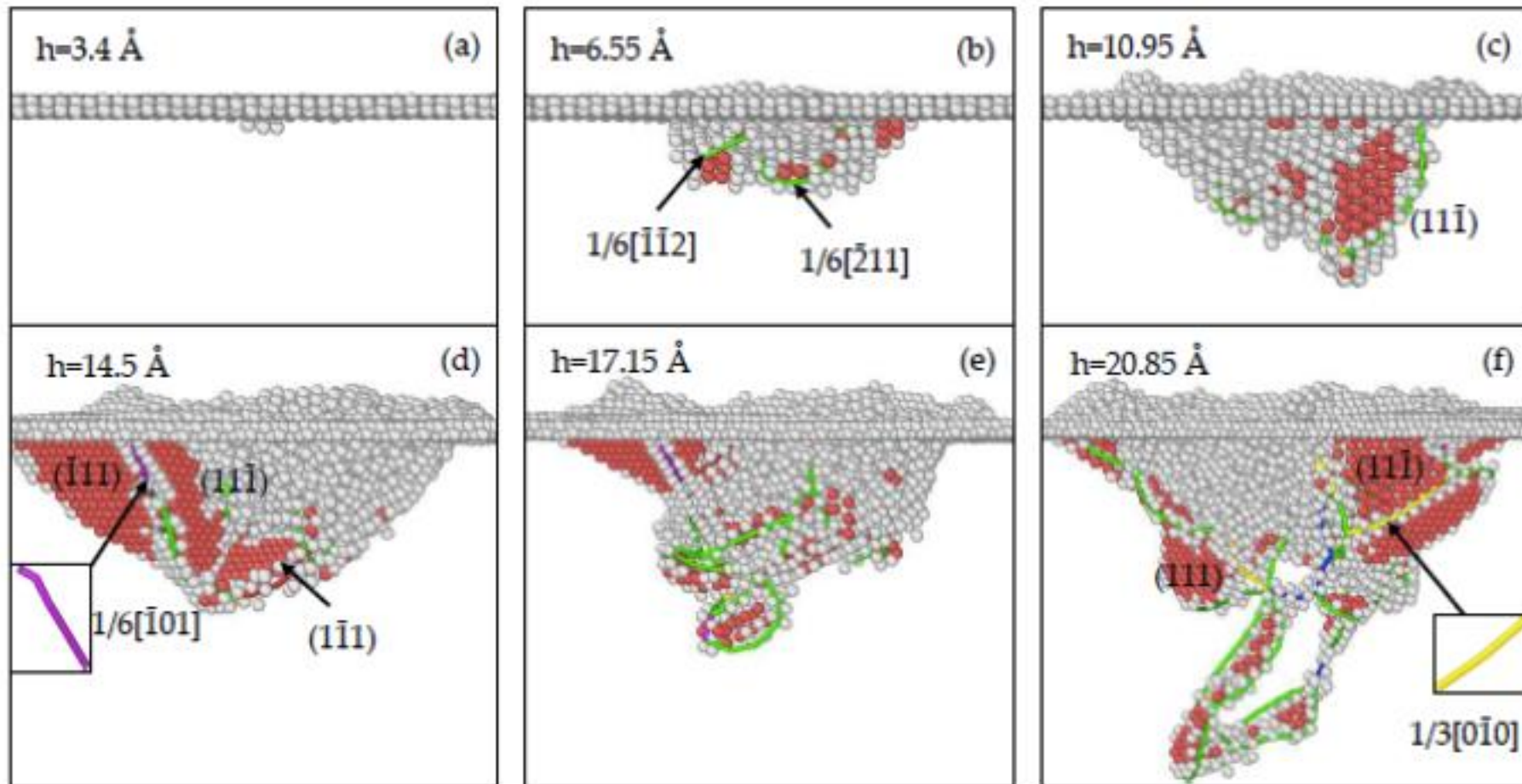


Figure 4. Defect evolution in the (100) sample during the loading process (a–g, c₀, e₀), and the unloading process (f–g). (SESF is the external stacking fault, TB is the twinning boundary).



Зарождение дефектов, образец (-110)



Зарождение дефектов, образец (-110)

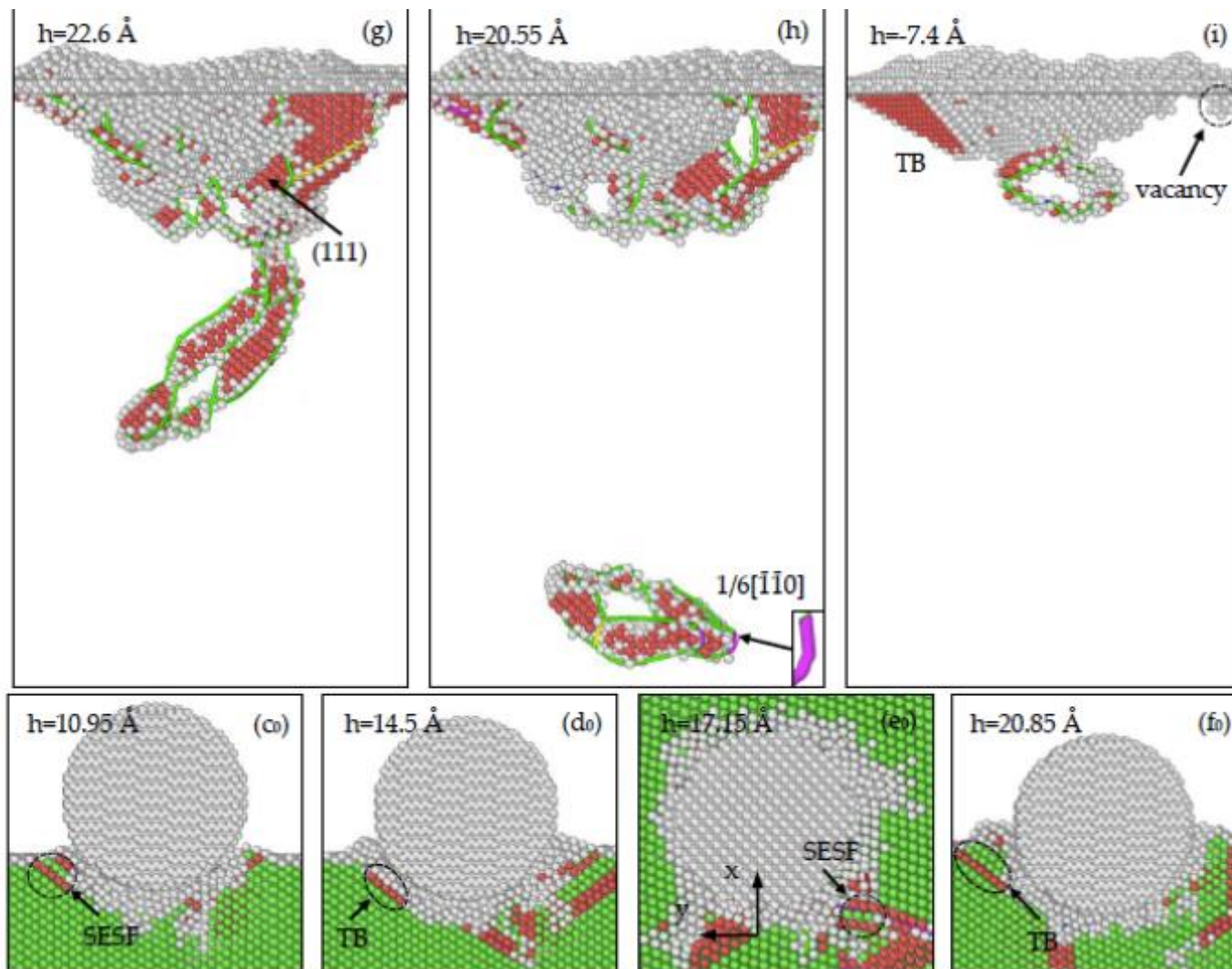
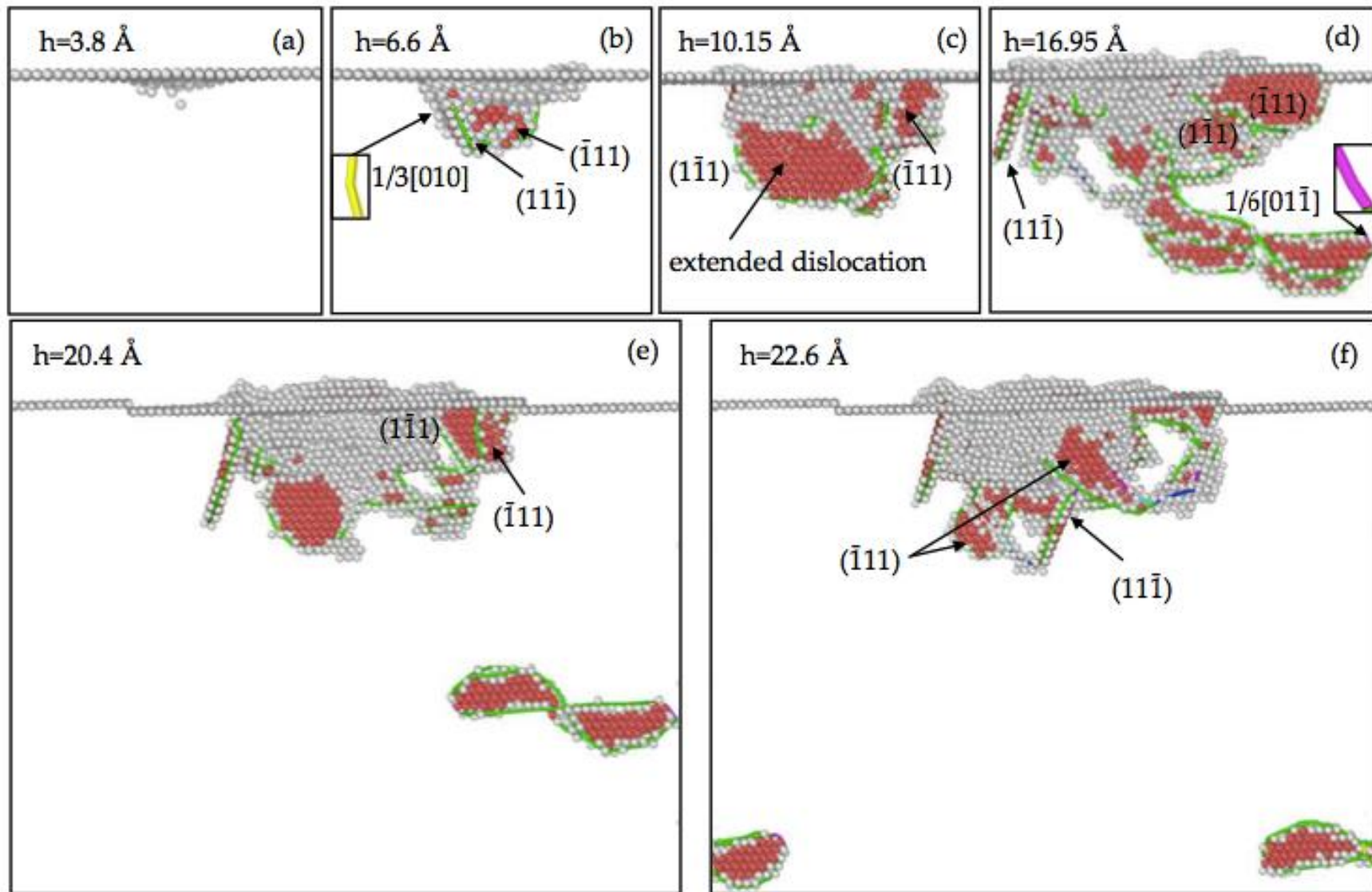


Figure 5. Defect evolution in the $(\bar{1}10)$ sample during the loading process (a-g, c₀-f₀), and the unloading process (h-i). (SESF is the external stacking fault, TB is the twinning boundary).



Зарождение дефектов, образец (111)



Зарождение дефектов, образец (111)

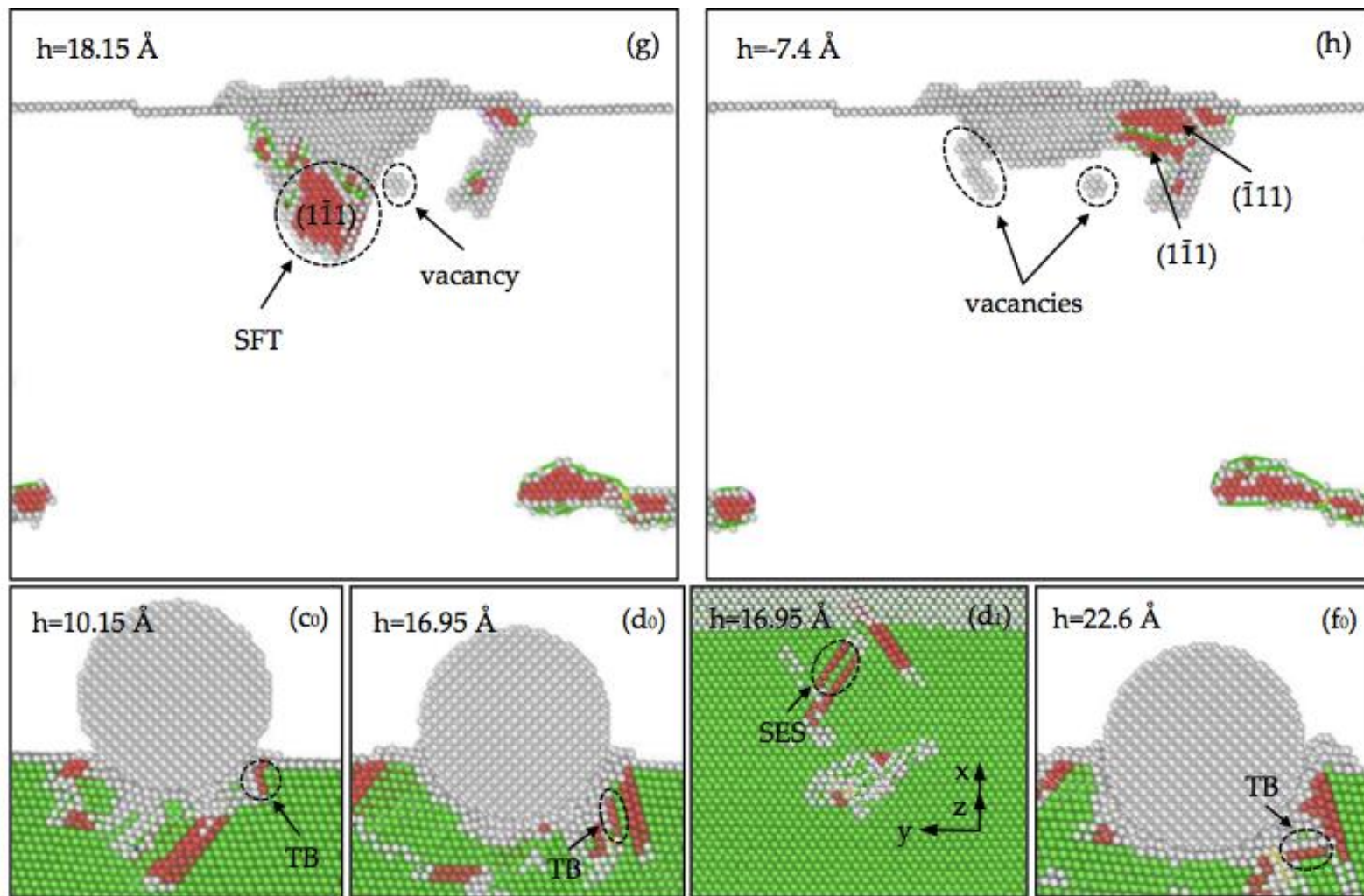


Figure 6. Defect evolution in the (111) sample during the loading process (a-f, c₀-f₀, d₁), and the unloading process (g-h). (SFT is the stacking fault tetrahedron.).



Расчет твердости и упругих модулей

Equations (2)–(6):

$$H = \frac{P_{\max}}{A_c} \quad (2)$$

$$A_c = \pi a^2 = \pi(2Rh_c - h_c^2) \quad (3)$$

$$h_c = h_{\max} - \varepsilon \frac{P_{\max}}{S} \quad (4)$$

$$S = \left. \frac{dp}{dh} \right|_{h=h_{\max}} \quad (5)$$

$$P = B(h - h_f)^m \quad (6)$$

where, P_{\max} is the load at the maximum depth, A_c is the contact area, R is the indenter radius, h_c is the contact depth, h_{\max} is the maximum depth, ε is the correction factor, and $\varepsilon = 0.75$ for the spherical indenter [51], fitting 25–50% of the incipient unloading curve with Equation (6) and the stiffness S is obtained by Equation (5), h_f is the indentation depth after unloading, B and m are fitting parameters.

Table 2. Values of hardness and elastic modulus for different samples.

Samples	(100)	(110)	(111)
Hardness (GPa)	6.42	6.63	6.91
Elastic modulus (GPa)	164.5	175.8	192.4



Выводы

In this paper, the effect of crystal orientation on the deformation mechanisms and mechanical properties of γ -TiAl during nanoindentation at 300 K was demonstrated by molecular dynamics simulations. The load-depth curve, the defect evolution process as well as the related mechanical parameters of different samples were analyzed. In particular, the following conclusions can be drawn:

- (1) During the loading process of each case, there is no pronounced pop-in event in the load-depth curve when the initial plastic deformation of γ -TiAl occurs, which can be explained by the dislocation nucleating before the first load drop.
- (2) During the unloading process of the (110) and (111) cases, there is a peak in both load-depth curves, because several dislocations move to the free surface and annihilate causing the release of energy.
- (3) Stacking faults (intrinsic stacking faults and extrinsic stacking faults), twin boundaries and vacancies are generated in all cases. While interstitials are formed only in the (100) sample; a stacking fault tetrahedron is formed in the (111) sample; and a prismatic dislocation loop is formed in both the (110) and (111) samples.



Выводы

(4) For the (110) sample, the prismatic dislocation loop moves to the upper free surface and shrinks with the rise of the indenter. However, for the (111) sample, the prismatic dislocation loop continues to glide downward with the indenter returning and finally dissociates into two parts adhering on the side surfaces of the substrate, which is caused by the periodic boundary condition.

(5) The values of the critical load, strain energy, elastic modulus and hardness for the (111) sample are the maximal, and those for the (100) sample are the minimal. These differences are attributed to the bond strength of atoms and the ease of crystal slip in different samples. Besides, the orientation dependence of the elastic modulus is greater than the hardness and critical load.

